J|A|C|S
ARTICLES
Published on Web 11/08/2006

Determination of the Adsorption Isotherm of Methanol on the Surface of Ice. An Experimental and Grand Canonical Monte Carlo Simulation Study

Pál Jedlovszky,*,† Lívia Pártay,† Paul N. M. Hoang,‡ Sylvain Picaud,‡ Philipp von Hessberg,§ and John N. Crowley§

Contribution from the Laboratory of Interfaces and Nanosize Systems, Institute of Chemistry, Eötvös Loránd University, Pázmány Péter stny. 1/a, H-1117 Budapest, Hungary, Laboratoire de Physique Moléculaire—UMR CNRS 6624, Faculté des Sciences, Université de Franche-Comté, F-25030 Besançon Cedex, France, and Division of Atmospheric Chemistry, Max-Planck-Institut für Chemie, Postfach 3060, D-55020 Mainz, Germany

Received August 1, 2006; E-mail: pali@chem.elte.hu

Abstract: The adsorption isotherm of methanol on ice at 200 K has been determined both experimentally and by using the Grand Canonical Monte Carlo computer simulation method. The experimental and simulated isotherms agree well with each other; their deviations can be explained by a small (about 5 K) temperature shift in the simulation data and, possibly, by the non-ideality of the ice surface in the experimental situation. The analysis of the results has revealed that the saturated adsorption layer is monomolecular. At low surface coverage, the adsorption is driven by the methanol−ice interaction; however, at full coverage, methanol−methanol interactions become equally important. Under these conditions, about half of the adsorbed methanol molecules have one hydrogen-bonded water neighbor, and the other half have two hydrogen-bonded water neighbors. The vast majority of the methanols have a hydrogen-bonded methanol neighbor, as well.

1. Introduction

Interest in the interactions between trace gases and ice surfaces has been stimulated in recent decades by the recognition of the crucial role that ice surfaces can play in catalytic ozone destruction resulting from halogen activation in the polar stratosphere[1,2] and, more recently, in partitioning of photochemically active trace gases from the gas phase to the ice phase.[3,4]

Because of their known impact on the stratospheric ozone hole, many experimental studies of trace gas−ice interactions have focused on strong inorganic acidic gases such as HCl and HNO_3 (see, for example, the recent reviews by Abbatt[5] and Huthwelker[6]). The important role of volatile organic compounds (VOC) as important sources for HO*x* radicals in the upper troposphere has only recently been established, and the potential for VOC−ice interactions to modify photochemical HO*x* production has been the subject of recent attention.

In a series of experiments, Sokolov and Abbatt have investigated the adsorption of different alcohols on ice, between 213 and 245 K, as a function of their size (from ethanol to 1-hexanol)[7] by using a coated-wall flow tube coupled to a mass spectrometer. Their results show that the saturated surface coverages are all within ±50% around the value of 5.0 μmol/m^2, which corresponds to monolayer-like coverages for alcohols. These results also suggest that the alkyl chains are aligned perpendicular to the surface at monolayer coverage. In order to characterize the influence of various organic functional groups (e.g., C═O, O−H, C(O)OH, C(O)H) on the interaction between VOCs and ice, the adsorption of acetone,[8,9] acetic acid,[7,10] formaldehyde,[11] methanol,[11,12] acetaldehyde,[12] and 2,3-butanedione[13] on ice has recently been investigated experimentally using either a Knudsen cell flow reactor or a coated-wall flow tube. These studies have shown that the interaction between VOCs and ice is of the simplest type, i.e., reversible physisorption, and that the amount of trace gas taken up on the surface is adequately described by a single-site Langmuir isotherm. The corresponding adsorption energies have been measured within the same range, i.e., between −70 and

† Eötvös Loránd University.
‡ Université de Franche-Comté.
§ Max-Planck-Institut für Chemie.

(1) Solomon, S.; Garcia, R. R.; Rowland, F. S.; Wuebbles, D. J. *Nature* **1986**, *321*, 755.
(2) Molina, M. *Oceanus* **1988**, *31*, 47.
(3) Lawrence, M. G.; Crutzen, P. J. *Tellus* **1998**, *50B*, 263.
(4) Popp, P. J.; et al. *Geophys. Res.* **2004**, *109*, D06302.
(5) Abbatt, J. P. D. *Chem. Rev.* **2003**, *103*, 4783.
(6) Huthwelker, T.; Ammann, M.; Peter, T. *Chem. Rev.* **2006**, *106*, 1375.
(7) Sokolov, O.; Abbatt, J. P. D. *J. Phys. Chem. A* **2002**, *106*, 775.
(8) Domine, F.; Rey-Hanot, L. *Geophys. Res. Lett.* **2002**, *29*, 1873.
(9) Bartels-Rausch T.; Guimbaud, C.; Gäggeler, H. W.; Ammann, M. *Geophys. Res. Lett.* **2004**, *31*, L16110.
(10) Picaud, S.; Hoang, P. N. M.; Peybernès, N.; Le Calvé, S.; Mirabel, P. *J. Chem. Phys.* **2005**, *122*, 194707.
(11) Winkler, A. K.; Holmes, N. S.; Crowley, J. N. *Phys. Chem. Chem. Phys.* **2002**, *4*, 5270.
(12) Hudson, P. K.; Zondlo, M. A.; Tolbert, M. A. *J. Phys. Chem. A* **2002**, *106*, 2882.
(13) Peybernès, N.; Marchand, C.; Le Calvé, S.; Mirabel, P. *Phys. Chem. Chem. Phys.* **2004**, *6*, 1277.

10.1021/ja065553+ CCC: $33.50

−50 kJ/mol, for all these organic molecules except for formaldehyde, for which no significant adsorption has been found.[11]

Despite these recent experimental studies, a detailed description of the molecular parameters that control, e.g., gas-to-ice partitioning or rates of surface accommodation is largely missing.[5] To some extent, this is due to the complexity of the ice surface, but it is also due to a lack of coverage of parameter space that enables a physical−chemical description of the interaction. Fundamental questions remain on how trace gases interact with ice, especially regarding their location on the ice surface and, e.g., the competition between hydrogen-bonding to ice and lateral hydrogen-bonding between adsorbed species. In a series of previous papers, molecular dynamics (MD) simulations have been used to investigate the adsorption of acetone,[14] methanol,[15] formaldehyde,[15] ethanol,[16] and acetic acid[10] on ice. Indeed, MD simulations allow a realistic modeling of the oxygenated VOC−ice interactions by making it possible to take into account a large number of molecules in the calculations, and by including temperature effects. The results of these simulations were in fair agreement with both experimental data[7,8,11,12] and ab initio calculations,[17] in particular regarding the adsorption energy and the saturation coverage.

In order to determine the full adsorption isotherm of such VOC molecules on ice at tropospheric conditions, the Grand Canonical Monte Carlo (GCMC) simulation method[18,19] seems to be a particularly suitable tool. Indeed, this method allows one to simulate an adsorption experiment by keeping the temperature constant and controlling the chemical potential of the adsorbed molecules (or the pressure of the corresponding gas). By varying the chemical potential, GCMC allows the theoretical characterization of the adsorption isotherm and its comparison with experimental data. This method has been successfully used to simulate adsorption on fixed substrates, such as carbonaceous materials,[20−25] silica,[26,27] or MgO substrates.[28] However, in spite of the rapidly growing literature of simulation studies of ice,[29−42] to our knowledge, GCMC has never previously been used to determine an adsorption isotherm on a mobile molecular substrate such as an ice surface.

In the present paper, we present results of GCMC calculations as well as of an adsorption experiment using the coated-wall flow tube technique for the determination of the adsorption isotherm of methanol on ice at 200 K. This combined theoretical and experimental study aims at furthering our understanding of such trace gas−ice interactions beyond what can be achieved by either experiment or theory alone. The choice of methanol is dictated by the possibility of getting high-quality, reproducible experimental data on this system.[11] Moreover, from a theoretical point of view, its interaction with water is well described by simple potential models that have been proved to yield accurate theoretical results with respect to experimental data.[15] Besides determining the adsorption isotherm, we also present here a detailed analysis of the energy and surface orientation of the adsorbed methanol molecules at various surface coverage values on the basis of the GCMC simulation results.

2. Methods

2.1. Experimental Details. The experimental method used was similar to that reported already from this laboratory,[11] so only a short description of the most pertinent features is given. The ice surfaces, available as thin films (50−100 μm), which coated the inner surface of a thermostatted, low-pressure, laminar flow tube, were prepared by freezing a few milliliters of distilled water at 258 K, which evenly coated the reactor wall. Subsequent to freezing at 258 K, the film was cooled to 200 K and an appropriate flow of H_2O added to the gas phase to prevent evaporation during the experiment. Films prepared this way were translucent to the eye and are considered to be sufficiently smooth that the geometric and surface areas are the same. This assumption is supported by observations of similar uptake characteristics of a number of different gases on ice surfaces prepared this way.[5] Methanol, diluted in He, was introduced into the reactor via a moveable injector, which allowed variation of the ice surface area to be exposed to methanol. For all results reported here, the injector was moved 10 cm, exposing about 80 cm^2 of ice surface. The amount of methanol taken up to the surface at equilibrium was derived by integration of the calibrated, gas-phase methanol signal over the exposure time. This was defined as the time taken for the methanol signal to return to its original value before exposure, i.e., when the rates of adsorption and desorption are equal and the net uptake is zero. Methanol was detected as its parent ion in the gas phase (He at 1 Torr) using modulated molecular beam mass spectrometry with electron impact ionization. Whereas previous experiments explored the linear part of the Langmuir isotherm for methanol−ice interactions, the present experiments extend upward the range of methanol concentrations so that comparisons between theory and experiment both at low and maximum surface coverages could be made.

2.2. Monte Carlo Simulations. In order to calculate the adsorption isotherm, a series of Monte Carlo simulations has been performed on the grand canonical (μ,*V*,*T*) ensemble at 200 K. The *X*, *Y*, and *Z* edges of the rectangular basic simulation box have been kept fixed at 100, 35.926, and 38.891 Å, respectively. Standard periodic boundary conditions have been applied. In the middle of the basic simulation box along the *X*-axis have been placed 18 molecular layers of proton-disordered I_h ice, containing 160 water molecules per layer. These layers are then parallel with the *YZ* plane of the basic box. At the beginning of the simulations, the water molecules formed a perfect ice I_h crystal. (The lengths of the *Y* and *Z* axes have been set according to the

(14) Picaud, S.; Hoang, P. N. M. *J. Chem. Phys.* **2000**, *112*, 9898.
(15) Collignon, B.; Picaud, S. *Chem. Phys. Lett.* **2004**, *393*, 457.
(16) Peybernès, N.; Le Calvé, S.; Mirabel, P.; Picaud, S.; Hoang, P. N. M. *J. Phys. Chem. B* **2004**, *108*, 17425.
(17) Marinelli, F.; Allouche, A. *Chem. Phys.* **2001**, *272*, 137.
(18) Adams, D. J. *Mol. Phys.* **1975**, *29*, 307.
(19) Allen, M. P.; Tildesley, D. J. *Computer Simulation of Liquids*; Clarendon Press: Oxford, 1987.
(20) Muller, E. A.; Rull, L. F.; Vega, L. F.; Gubbins, K. E. *J. Phys. Chem.* **1996**, *100*, 1189.
(21) Muller, E. A.; Gubbins, K. E. *Carbon* **1998**, *36*, 1433.
(22) Muller, E. A.; Hung, F. R.; Gubbins, K. E. *Langmuir* **2000**, *16*, 5418.
(23) Brennan, J. K.; Bandosz, T. J.; Thomson, K. T.; Gubbins, K. E. *Colloids Surf. A* **2001**, *187*−*188*, 539.
(24) Stirolo, A.; Chialvo, A. A.; Gubbins, K. E.; Cummings, P. T. *J. Chem. Phys.* **2005**, *122*, 234712.
(25) Moulin, F.; Picaud, S.; Hoang, P. N. M.; Pártay, L.; Jedlovszky, P. *Mol. Simul.* **2006**, *32*, 487.
(26) Puibasset, J.; Pellenq, R. J. M. *J. Chem. Phys.* **2003**, *118*, 5613.
(27) Puibasset, J.; Pellenq, R. J. M. *J. Chem. Phys.* **2005**, *122*, 094704.
(28) Daub, C. D.; Patey, G. N.; Jack, D. B.; Sallabi, A. K. *J. Chem. Phys.* **2006**, *124*, 114706.
(29) Brodholt, J.; Sampoli, M.; Vallauri, R. *Mol. Phys.* **1995**, *85*, 81.
(30) Buch, V.; Delzeit, L.; Blackledge, C.; Devlin, J. C. *J. Phys. Chem.* **1996**, *100*, 3732.
(31) Rick, S. W. *J. Chem. Phys.* **2001**, *114*, 2276.
(32) Hayward, J. A.; Haymet, A. D. J. *Phys. Chem. Chem. Phys.* **2002**, *4*, 3712.
(33) Grishina, N.; Buch, V. *J. Chem. Phys.* **2004**, *120*, 11200.
(34) Bryk, T.; Haymet, A. D. J. *Mol. Simul.* **2004**, *30*, 131.
(35) Rick, S. W. *J. Chem. Phys.* **2005**, *122*, 0945041.
(36) Abascal, J. L. F.; Sanz, E.; Garcia Fernández, R.; Vega, C. *J. Chem. Phys.* **2005**, *122*, 234511.
(37) Vega, C.; McBride, C.; Sanz, E.; Abascal, J. L. F. *Phys. Chem. Chem. Phys.* **2005**, *7*, 1450.
(38) Vega, C.; Abascal, J. L. F. *J. Chem. Phys.* **2005**, *123*, 144504.
(39) Baranyai, A.; Bartók, A.; Chialvo, A. A. *J. Chem. Phys.* **2005**, *123*, 054502.
(40) Baranyai, A.; Bartók, A.; Chialvo, A. A. *J. Chem. Phys.* **2006**, *124*, 074507.
(41) Buch, V.; Martonak, R.; Parrinello, M. *J. Chem. Phys.* **2006**, *124*, 204705.
(42) Knight, C.; Singer, S. J.; Kuo, J. L.; Hirsch, T. K.; Ojame, L.; Klein, M. L. *Phys. Rev. E* **2006**, *73*, 056113.

Table 1. Data of the Adsorption Isotherm of Methanol on Ice, As Obtained from Our Simulations

B	μ/kJ mol^{-1}	$\langle N \rangle$	Γ/μmol m^{-2}	p/p_0
−3.0	−32.29	883.1		
−4.0	−33.95	866.6		
−4.2	−34.28	865.5		
−4.4	−34.61	862.6		
−4.6	−34.95	862.3		
−4.8	−35.28	859.3		
−5.0	−35.61	570.9	33.92	1.000
−5.2	−35.94	229.9	13.66	0.819
−5.5	−36.44	187.3	11.13	0.607
−5.8	−36.94	176.3	10.47	0.450
−6.2	−37.61	170.0	10.10	0.301
−6.5	−38.11	165.8	9.85	0.223
−6.8	−38.61	163.3	9.70	0.165
−7.2	−39.27	159.3	9.47	0.111
−7.6	−39.94	155.5	9.24	7.43×10^{-2}
−8.0	−40.60	151.2	8.98	4.98×10^{-2}
−8.5	−41.43	144.7	8.60	3.02×10^{-2}
−9.0	−42.26	138.1	8.21	1.83×10^{-2}
−9.2	−42.60	134.0	7.96	1.50×10^{-2}
−9.4	−42.93	127.1	7.55	1.23×10^{-2}
−9.6	−43.26	114.8	6.82	1.01×10^{-2}
−9.8	−43.59	115.8	6.88	8.24×10^{-3}
−10.0	−43.92	99.1	5.89	6.74×10^{-3}
−10.2	−44.26	88.4	5.25	5.52×10^{-3}
−10.6	−44.92	59.9	3.56	3.7×10^{-3}
−11.0	−45.59	44.6	2.65	2.48×10^{-3}
−11.2	−45.92	42.3	2.52	2.03×10^{-3}
−11.6	−46.59	26.3	1.56	1.36×10^{-3}
−12.0	−47.25	23.5	1.40	9.13×10^{-4}
−13.0	−48.91	11.3	0.67	3.36×10^{-4}
−14.0	−50.58	6.80	0.41	1.24×10^{-4}
−15.0	−52.24	3.60	0.21	4.54×10^{-5}
−16.0	−53.90	1.72	0.10	1.67×10^{-5}

geometry of this crystal.) The water molecules have been described by the five-site TIP5P model,[43] which is known to be frozen below 274 K.[38]

The number of methanol molecules, described by the six-site potential model of Jorgensen and Madura,[44] has been left to fluctuate around the equilibrium value that corresponds to their chemical potential μ in the system. In order to control the chemical potential of the methanol molecules, the B parameter of Adams,[18] related to the chemical potential through the equation[19]

$$\mu = k_B T\left(B + \ln \frac{\Lambda^3}{V}\right) \quad (1)$$

has been kept constant in the simulation. In this equation, Λ denotes the thermal de Broglie wavelength of methanol,

$$\Lambda = \frac{h}{\sqrt{2\pi k_B T m}}, \quad (2)$$

where m is the mass of the methanol molecule. The simulations have been repeated with 33 different values of B, ranging from −3 to −16, corresponding to μ values falling in the range between −32.3 and −53.9 kJ/mol. The B and μ values corresponding to the simulations we performed are summarized in Table 1.

The simulations have been done using the program MMC.[45] In the simulations, particle displacement and insertion/deletion moves have been performed in an alternating order. In a particle displacement step, a randomly chosen molecule has been randomly translated by no more than 0.25 Å and randomly rotated around a randomly chosen space-fixed axis by no more than 15°. Water and methanol molecules have been selected for particle displacement moves in an alternating order, but the molecules belonging to the innermost two layers of ice have been kept fixed during the entire course of the simulation. The methanol insertion/deletion steps have been done using the cavity-biased scheme of Mezei.[46,47] Insertion and deletion attempts have been performed with equal probabilities. Only insertions into cavities of the minimum radius of 2.5 Å have been attempted. Suitable cavities have been searched for along a 100 × 100 × 100 grid, which has been regenerated after every 10^6 Monte Carlo steps. In order to remove the bias introduced into the sampling by attempting insertions solely into suitably large cavities, the acceptance criterion of the insertion/deletion moves has to be corrected by the factor of $\ln P^N_{cav}$,[46,47] where P^N_{cav} is the probability of finding a suitable cavity in the system containing N methanol molecules. The value of P^N_{cav} has been determined simply as the ratio of the cavities found and grid points checked in the configurations containing N methanols.

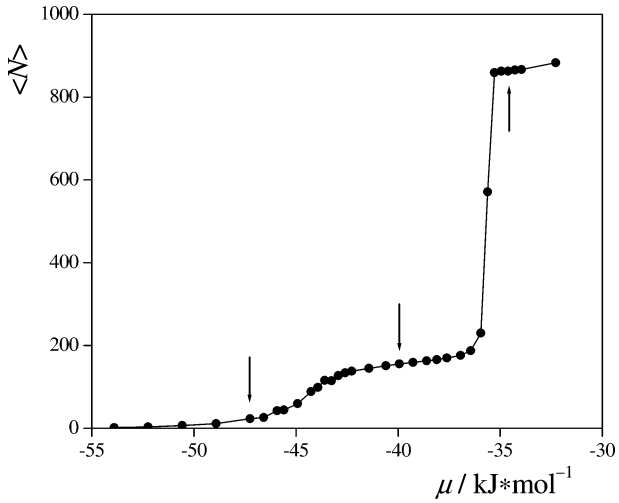

Figure 1. Average number of methanol molecules in the basic simulation box as a function of the methanol chemical potential. Arrows indicate the systems used in the detailed analyses.

In the simulations, all interactions have been truncated to zero beyond the molecule-based cutoff distance of 12.5 Å. In accordance with the original parametrization of the potential models used,[43,44] no long-range correction has been applied for the electrostatic interactions. The systems have been equilibrated by performing 10^8 Monte Carlo moves. The number of the methanol molecules present in the system has then been averaged over 2×10^8 equilibrium configurations. Finally, in three of the systems simulated, characterized by the B values of −4.4, −7.6, and −12.0, respectively, 2500 sample configurations, separated by 4×10^4 Monte Carlo moves each, have been saved for further analyses.

3. Results and Discussion

3.1. Adsorption Isotherm. The adsorption isotherm obtained from the simulation, i.e., the average number of methanol molecules present in the simulation box $\langle N \rangle$ as a function of the methanol chemical potential μ, is plotted in Figure 1; the μ and $\langle N \rangle$ values are also summarized in Table 1. The calculated $\langle N \rangle(\mu)$ isotherm shows two sharply increasing regions and two plateaus. At low μ values, the isotherm exhibits an exponential increase up to about $\mu = -43$ kJ/mol. This part of the isotherm corresponds to the building up of the adsorption layer. Above this μ value, the adsorption layer becomes saturated; large changes in the chemical potential result in only a rather small increase of the number of adsorbed molecules in this region. The number of adsorbed molecules found at this plateau region

(43) Mahoney, M.; Jorgensen, W. L. *J. Chem. Phys.* **2000**, *112*, 8910.
(44) Jorgensen, W. L.; Madura, J. D. *J. Am. Chem. Soc.* **1983**, *105*, 1407.
(45) Mezei, M. MMC Program, available at http://inka.mssm.edu/~mezei/mmc.
(46) Mezei, M. *Mol. Phys.* **1980**, *40*, 901.
(47) Mezei, M. *Mol. Phys.* **1987**, *61*, 565; **1989**, *67*, 1207 (erratum).

of the isotherm corresponds to an average surface area per molecule of about 20 Å^2, indicating that the saturated adsorption layer is probably monomolecular. Finally, at a μ value of about −35.5 kJ/mol, the isotherm exhibits a sudden jump, corresponding to the condensation of methanol. Above this chemical potential, the box is already filled with methanol molecules; the resulting density of the methanol phase is about 0.89 g/cm^3, which agrees to within 5% with the experimental density of liquid methanol at 193 K.[48]

In order to compare the simulated isotherm with the experimental data, we have converted the obtained $\langle N\rangle(\mu)$ curve to the isotherm in the $\Gamma(p_{rel})$ form. The surface density of methanol, Γ, has been calculated simply by dividing the average number of methanols in the system by the total surface area of the ice phase. The relative pressure of the vapor phase, p_{rel}, i.e., the pressure normalized by the pressure of the saturated vapor p_0, has been calculated as

$$p_{rel} = \frac{p}{p_0} = \frac{\exp B}{\exp B_0}, \tag{3}$$

using the relation[28]

$$B = \ln \frac{pV}{k_B T}. \tag{4}$$

In eq 3, the value of $B_0 = -5$ has been used, i.e., the B value at which the condensation of methanol occurs, and hence the liquid and vapor phases of methanol are in equilibrium. Obviously, eqs 3 and 4 can only be used in the vapor phase, i.e., for $p_{rel} \leq 1$, and thus the full $\langle N\rangle(\mu)$ curve has only been converted to the $\Gamma(p_{rel})$ form up to the point of condensation. The p_{rel} and Γ values corresponding to the simulations performed are also listed in Table 1.

The calculated $\Gamma(p_{rel})$ isotherm is compared with the experimental curve in Figure 2a. For completeness, besides the results of the present measurement, the data points of our previous experiment,[11] performed at lower pressures at 198 K, are also indicated. The two experimental data sets match very well with each other, as may be expected given that the experiments were very similar. As described previously,[11] the experimental data are described rather well by a Langmuir isotherm, which is characterized by a linear dependence of the surface coverage on methanol concentration at low partial pressures of methanol, which levels off as N (the number of molecules on the surface) approaches N_{max}:

$$\frac{N}{N_{max}} = \frac{pK_{methanol}}{pK_{methanol} + 1}, \tag{5}$$

where $K_{methanol}$ is the Langmuir partitioning constant and p is the methanol pressure.

In our previous work, we examined the isotherm at low methanol partial pressures and derived a value of $N_{max} = 5.3 \pm 1.7$ μmol/m^2. The present study was conducted using higher partial pressures of methanol and returned a value of $N_{max} = 7.0 \pm 1.0$ μmol/m^2, somewhat larger but, within experimental uncertainty, still in agreement with our previous result. At this point it is useful to examine the assumptions that are inherent in the Languir equation: that all adsorptrion sites are equal and

(48) Yamaguchi, T.; Hidaka, K.; Soper, A. K. *Mol. Phys.* **1999**, *96*, 1159.

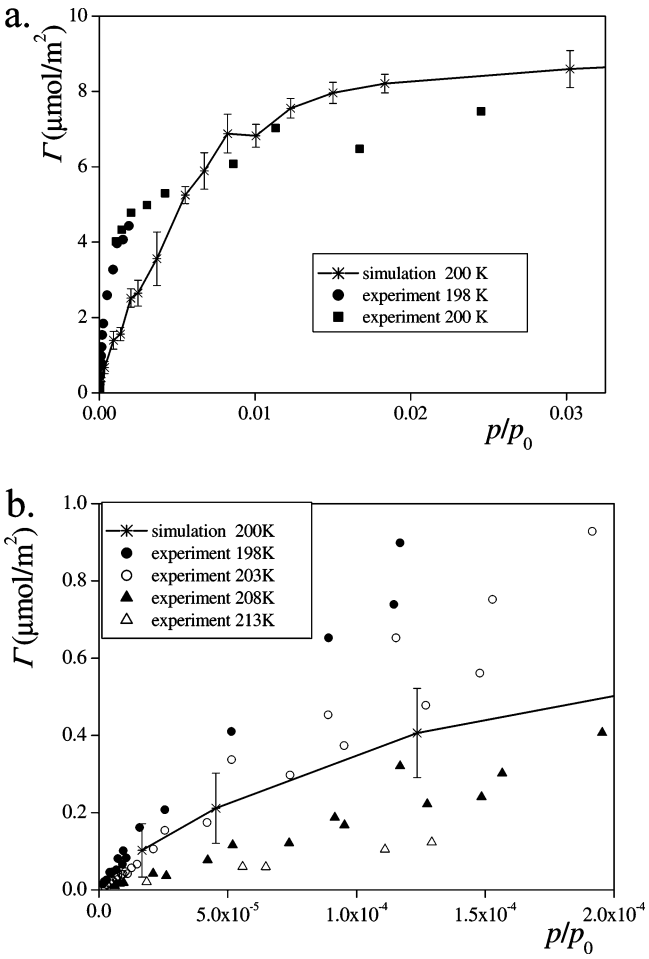

Figure 2. (a) Adsorption isotherm of methanol on ice, as obtained from our simulation (∗) and experiment (■). Results of our previous experiment performed at 198 K[11] are also indicated (●). (b) The very low pressure part of the simulated isotherm, together with results of our previous experiments performed at 198 (●), 203 (○), 208 (▲), and 213 K (△).[11] The lines connecting the simulated data points are just guides to the eye. The estimated uncertainty of the simulated values is indicated by the error bars.

that, even at high coverage, there are no lateral interactions. A close examination of the experimental data in Figure 2 reveals a slightly increasing value of N even at the highest coverage, suggesting breakdown of the Langmuir isotherm under these conditions. Most interestingly, the simulations also show this behavior, which, as discussed below, is due to strong lateral interactions between adsorbed methanol molecules. Clearly, N_{max} is a poorly defined (perhaps even meaningless) parameter in experimental studies of trace gas−ice interactions for which adsorbate−adsorbate interactions are possible.

Although differences are apparent, certain aspects of the experimental and simulated curves agree reasonably well with each other. In particular, the simulated p_{rel} value at which the saturation of the adsorption layer occurs is in the same order of magnitude (i.e., about 30% larger) as the experimental value; also, the experimental surface density of the saturated adsorption layer is well reproduced by the simulation. The most important difference between the two curves is that the linear, rising part of the experimental isotherm is noticeably steeper than that of the simulated curve. (This difference leads also to the aforementioned slight overestimation of the saturation pressure of the adsorption layer by the simulation.) In order to understand the origin of this deviation, we have enlarged the very low p_{rel}

part of the isotherms in Figure 2b. The results of our previous measurements, performed at somewhat higher temperatures,[11] are also indicated in this figure. It is evident that the slope of the linear part of the isotherm decreases with increasing temperature. It is also seen from the figure that the simulated curve, calculated at 200 K, consistently falls between the experimental isotherms obtained at 203 and 208 K, indicating that the apparent deviation between the simulated and experimental isotherms (Figure 2a) can simply be attributed to this slight (about 5 K) temperature shift in the simulation data. Such a shift of the thermodynamic properties of a system on the $p-T$ plane frequently occurs in computer simulations.[35−37,49,50] In our case, this observed temperature shift is probably due to a slight underestimation of the strength of the interaction between water and methanol, with respect to that of the methanol−methanol interaction. A potential other reason for this slight shift could be the fact that, in the simulations, contrary to the experimental situation, a perfect I_h ice surface has been used. Taking these considerations into account, the reproduction of the experimental isotherm by the simulation can be regarded as excellent.

3.2. Characterization of the Adsorption Layer. We have analyzed the properties of the adsorption layer in detail at three different chemical potential values: −47.25 kJ/mol, corresponding to low surface coverage; −39.94 kJ/mol, corresponding to the saturated adsorption layer; and −34.61 kJ/mol, corresponding to condensed methanol. An instantaneous snapshot of each of these three systems is shown in Figure 3.

The number density profiles of the methanol molecules as obtained in these three systems are shown in Figure 4. (In the calculation of these profiles, the methanol molecules have been represented by their centers of mass.) The number density profile of water in the $\mu = -47.25$ kJ/mol system is also indicated. All the profiles shown have been averaged over the two interfaces present in the basic simulation box. The peaks corresponding to the nine layers of ice are clearly separated by a distance of about 3.7 Å. Similar layering is observed in the condensed methanol phase, where four consecutive molecular layers can be distinguished. The methanol density profile in the $\mu = -39.94$ kJ/mol system coincides with the peak of the first methanol layer in the condensed methanol phase and drops to zero right after this peak, indicating that the saturated adsorption layer of methanol is indeed monomolecular.

Figure 5 shows the number density profiles of the C, O, and hydroxylic H atoms of the methanol molecules in the $\mu = -39.94$ kJ/mol system. It is clear that, among these three atoms, the H atom of the hydroxylic group is, on average, considerably closer to the ice surface than the other two atoms, whereas the C atom is considerably farther from the ice surface. This fact already provides some indication of the preferred orientation of the methanol molecules. This point will be further investigated in detail later in this section.

Energetics of the Adsorption. In order to investigate the energetics of the adsorption, we have calculated the binding energy of the methanol molecules at the ice surface, U_b (i.e., the energy of the interaction of the adsorbed methanol molecules with the rest of the system). We have also calculated the contributions to U_b from the interactions with the ice phase and

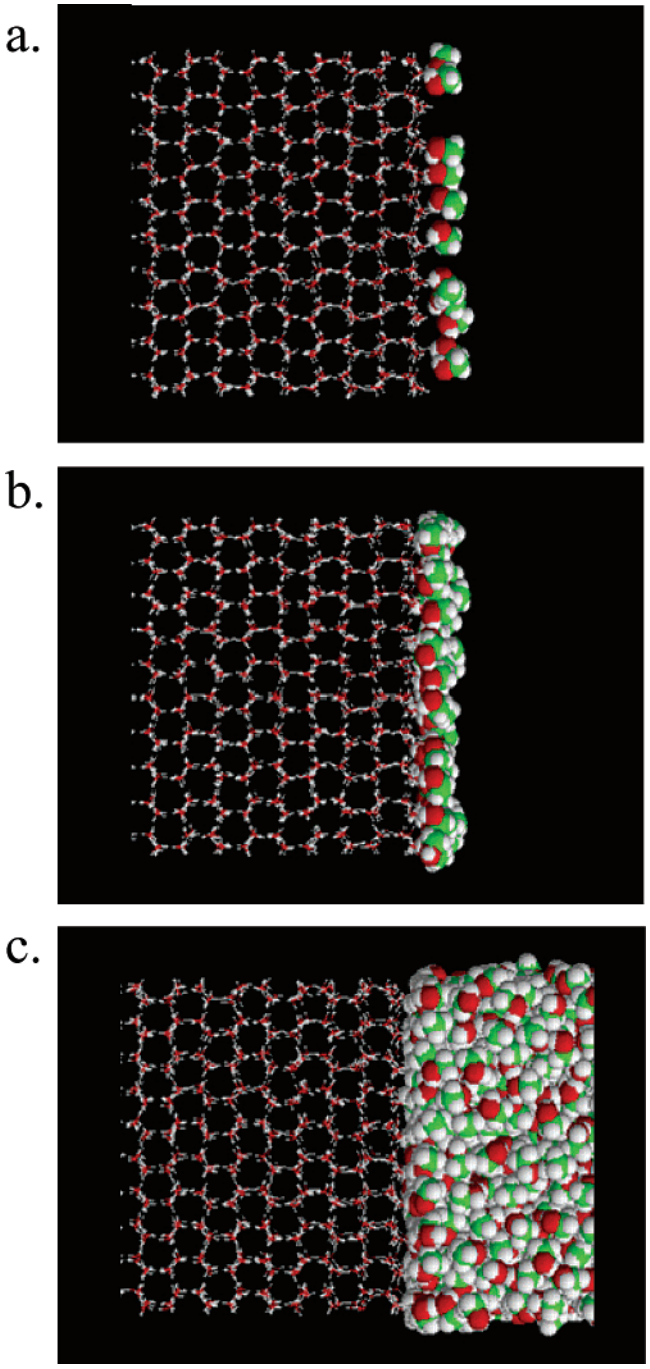

Figure 3. Instantaneous snapshot of the ice surface with the adsorbed methanol molecules in three of the simulated systems: (a) $\mu = -47.25$ kJ/mol ($B = -12.0$), (b) $\mu = -39.94$ kJ/mol ($B = -7.6$), and (c) $\mu = -34.61$ kJ/mol ($B = -4.4$).

with the other methanol molecules (U_b^{ice} and U_b^{met}, respectively). The distribution of the U_b, U_b^{ice}, and U_b^{met} energies is shown in Figure 6, as determined in the $\mu = -47.25$ kJ/mol system (i.e., at low surface coverage) and with $\mu = -39.94$ kJ/mol (i.e., at full coverage of the surface by a monolayer). As is seen, at low surface coverage the dominant contribution to U_b comes from the interaction of the adsorbed methanol molecule with the ice phase, whereas at full coverage the methanol−methanol energy term becomes comparable with the ice−methanol term. The $P(U_b^{met})$ distribution shows three peaks at low surface coverage. The dominant peak, at nearly zero energy, reflects the isolated methanol molecules, i.e., those

(49) Poole, P. H.; Sciortino, F.; Essmann, U.; Stanley, H. E. *Phys. Rev. E* **1993**, *48*, 3799.
(50) Jedlovszky, P.; Valauri, R. *Phys. Rev. E* **2003**, *67*, 011201.

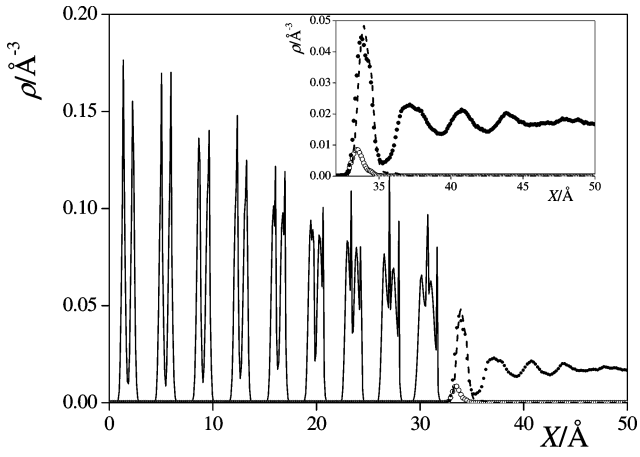

Figure 4. Molecular number density profiles of water in the $\mu = -47.25$ kJ/mol system (—) and methanol in the $\mu = -34.61$ kJ/mol (●), $\mu = -39.94$ kJ/mol (- - -), and $\mu = -47.25$ kJ/mol (○) systems. The inset shows the methanol density profiles on a magnified scale. All profiles shown are symmetrized over the two interfaces present in the basic simulation box.

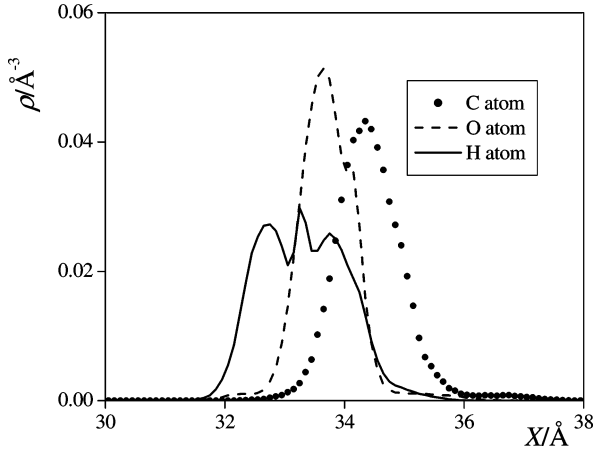

Figure 5. Number density profile of the C (●), O (- - -), and hydroxylic H (—) atoms of the methanol molecules in the $\mu = -39.94$ kJ/mol system.

having no methanol neighbors at the surface. The second peak, appearing as a shoulder at about −5 kJ/mol, i.e., at the low-energy side of the first peak, is due to the methanol molecules that have methanol neighbors but do not form hydrogen bonds with them, whereas the third peak, at about −21 kJ/mol, corresponds to methanols having a hydrogen-bonded methanol neighbor. The integration of the $P(U_b^{met})$ distribution up to the minimum following this peak reveals that only about 32% of the adsorbed methanol molecules are hydrogen-bonded to another methanol in this system.

At full coverage of the ice surface, the $P(U_b^{met})$ curve is already unimodal, exhibiting a single peak at −32 kJ/mol. This means that, in this case, all the methanol molecules are hydrogen-bonded to another methanol. Further, this peak appears at about 11 kJ/mol lower energies than the hydrogen-bonding peak of $P(U_b^{met})$ at low coverage, indicating that, upon saturation, not only does the average number of methanol−methanol hydrogen bonds per molecule increase, but these bonds also become considerably stronger.

On the other hand, an opposite trend can be observed for the methanol−water hydrogen bonds. At low surface coverage, the $P(U_b^{ice})$ distribution is bimodal. The first, small peak appears at about −31 kJ/mol, whereas the main peak of the distribution is located at −54 kJ/mol, i.e., close to twice the first value. Thus,

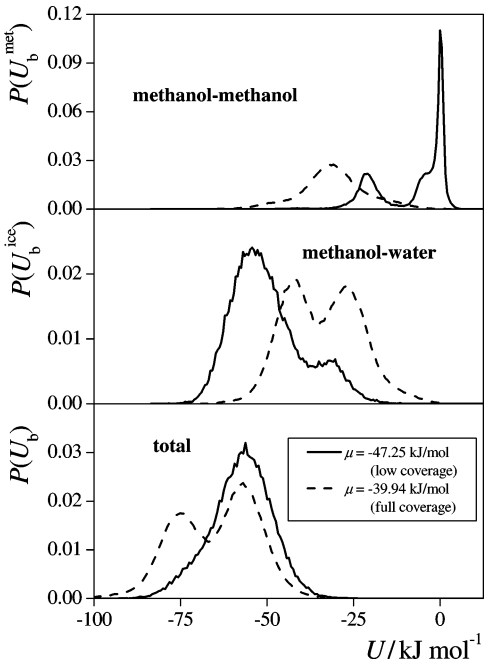

Figure 6. Distribution of the binding energy of an adsorbed methanol molecule (i.e., the energy of interaction between the adsorbed molecule and the rest of the system, bottom panel) and those of its contributions from the interaction of the methanol molecule with the ice phase (middle panel) and with the other methanol molecules (top panel). Solid lines, system at $\mu = -47.25$ kJ/mol (low surface coverage); dashed lines, system at $\mu = -39.94$ kJ/mol (full coverage).

the first peak can be attributed to methanols forming one hydrogen bond and the second peak to those forming two hydrogen bonds with the water molecules. By integrating the distribution up to the minimum between the two peaks, the fraction of the methanol molecules forming two hydrogen bonds with the ice phase is estimated to be about 87%.

The saturation of the adsorption layer does not change the bimodal character of $P(U_b^{ice})$; however, at full coverage, the two peaks become equally high, and both peaks are shifted to higher (i.e., less negative) energy values. The integration of $P(U_b^{ice})$ reveals that now 50% of the methanols form one hydrogen bond and 50% of them form two hydrogen bonds with the ice phase. Additionally, the shift of the peak position indicates that not only does the number of methanol−water hydrogen bonds per methanol molecule decrease when the adsorption layer gets saturated, but these hydrogen bonds also become weaker (i.e., presumably more distorted) than at low surface coverage.

The distribution of the full U_b energy is unimodal at low surface coverage but becomes bimodal at full coverage. Considering the fact that the first of the two peaks of $P(U_b)$ at full coverage appears at the same energy value (i.e., at about −56 kJ/mol) at which the only peak of $P(U_b)$ at low coverage is located, and also that this energy value is very close to the position of the second peak of $P(U_b^{ice})$, given by the methanols H-bonded twice to the ice phase at low coverage (i.e., −54 kJ/mol), we can conclude that, at low coverage, the vast majority of the methanol molecules form two hydrogen bonds with their neighbors. The lack of the second peak of $P(U_b)$ at about −30 kJ/mol indicates that the methanols having only one hydrogen-bonded water neighbor are usually also hydrogen-bonded to a methanol neighbor. On the other hand, the two

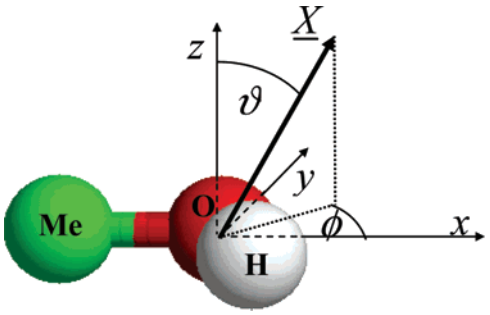

Figure 7. Definition of the local Cartesian coordinate frame fixed to the individual methanol molecules in order to describe their surface orientation. $\underline{X}$ is the surface normal vector pointing away from the ice phase, and ϑ and ϕ are its polar coordinates in this molecule-fixed local frame.

peaks of $P(U_b)$ at full coverage, appearing at −56 and −75 kJ/mol, are indicative of the methanols having two (i.e., one water and one methanol) and three (i.e., two waters and one methanol) hydrogen-bonded neighbors, respectively. The integration of the distribution up to the minimum between the two peaks reveals that the fractions of these two types of methanols are 60% and 40%, respectively.

Finally, it should be noted that the mean value of the $P(U_b^{ice})$ distribution in the $\mu = -47.25$ kJ/mol system (i.e., at low surface coverage) of −49.8 kJ/mol agrees very well with the experimental value of the heat of this adsorption, -51 ± 10 kJ/mol, measured at very low surface coverage, i.e., when the methanol−methanol contribution is negligibly small.[11]

Orientation of the Adsorbed Methanol Molecules. The facts that, upon saturation, the number of hydrogen-bonded methanol neighbors of an adsorbed methanol molecule increases and that of the hydrogen-bonded water neighbors decreases and, at the same time, the methanol−methanol hydrogen bonds become, on average, stronger and the methanol−water hydrogen bonds weaker must also be reflected in the orientational preferences of the adsorbed methanol molecules. Recently, we have shown that the surface orientation of a rigid molecule can only be unambiguously described by calculating the bivariate joint distribution of two independent orientational variables.[51,52] We have also demonstrated that the angular polar coordinates of the surface normal vector in a local coordinate frame fixed to the individual molecules are a suitable choice for these variables.[51,52] In defining this local frame here, we use the convention described in a previous paper.[53] Thus, the *x*-axis of this local frame coincides with the vector pointing from the C to the O atom of the methanol molecule. The *y*-axis lies also in the plane of the C atom and the O−H bond, with the *y* coordinate of the OH hydrogen atom being negative, whereas the *z*-axis is perpendicular to the above two axes. The choice of this local coordinate frame, together with the two polar angles ϑ and ϕ of the surface normal vector $\underline{X}$ (pointing away from the ice phase) in this frame, is illustrated in Figure 7. It should be noted that, for symmetry reasons, the angle ϑ should be in the range of $0 \le \vartheta \le 90°$ (given that the orientation of the methyl H atoms is disregarded). Further, since angle ϑ is formed by two spatial vectors, whereas ϕ is the angle between two vectors, restricted to lie in a given plane by definition, uncorrelated orientation of the methanol molecules with the ice surface corresponds to uniform distributions of $\cos\vartheta$ and ϕ.[53]

The bivariate distributions of the angular variables $\cos\vartheta$ and ϕ are shown in Figure 8, as obtained in the $\mu = -47.25$ and −39.94 kJ/mol systems (i.e., at low and full surface coverages, respectively) and also in the first methanol layer of the $\mu = -34.61$ kJ/mol system (condensed methanol). Each $\{\cos\vartheta,\phi\}$ point of these $P(\cos\vartheta,\phi)$ maps corresponds to a given orientation of the methanol molecule relative to the ice surface, and the value of $P(\cos\vartheta,\phi)$ gives the probability of occurrence of this orientation. As is seen, at low surface coverage two methanol orientations (denoted by I and II) are preferred; any intermediate orientation between these two occurs also with high probability, whereas the probability of the other orientations is negligible. In orientation I, the C−O−H plane of the molecule is perpendicular to the ice surface, whereas in orientation II this plane forms an angle of about 45° with the surface. In both of these orientations, the methyl group points to the vapor phase; however, in orientation I the O−H bond points flatly toward the ice phase, whereas in orientation II it points flatly away from the ice phase, as illustrated in Figure 8. At full coverage, peak I of the orientational map is shifted to lower ϕ values (i.e., to $\phi = 180°$). This peak is denoted here as I_a. The observed small shift of this peak upon saturation corresponds to a small rotation of the preferred alignment of the molecule within the plane perpendicular to the surface: in orientation I_a, the O−C bond stays perpendicular to the ice surface (see Figure 8). Contrary to the small shift of peak I, peak II slips, upon saturation, to a completely different point of the orientational map, which is characterized by the values $\cos\vartheta = 0.85$ and $\phi = 270°$. This peak, marked here as III, is now clearly separated from that of the other preferred orientation (i.e., I_a) of the methanol molecules by orientations of low probabilities. In orientation III, the C−O−H plane of the molecule forms an angle of about 30° with the ice surface in such a way that the C−O bond is roughly parallel with it and the O−H bond points as straight away from the ice surface within this plane as possible (i.e., it declines from the surface by about 30°, see Figure 8). Upon condensation of methanol, the preference of the molecules for alignment III almost completely disappears, and orientation I_a remains the only one clearly preferred.

In order to understand the origin of these orientational preferences of the adsorbed methanol molecules and relate them to the observed behavior of the binding energy distributions, we have to consider the fact that water molecules are aligned in four different orientations at the free surface of proton-disordered ice, I_h. These four water alignments, denoted by A−D, respectively, are illustrated in Figure 9. It is evident from Figures 8 and 9 that, in orientation I, methanol molecules can form two hydrogen bonds with the waters at the surface: one as an H-acceptor and another one as an H-donor, both of them with waters of either orientation A or D, as demonstrated in Figure 10. It should be noted that the preference of the molecules for this type of arrangement is also supported by the vibrational spectroscopy results of Huiskens et al., who have shown that a single methanol molecule adsorbed at the surface of medium-sized water clusters interacts with the waters both as a H-donor and as a H-acceptor.[54] On the other hand, methanols in

(51) Jedlovszky, P.; Vincze, Á.; Horvai, G. *J. Chem. Phys.* **2002**, *117*, 2271.
(52) Jedlovszky, P.; Vincze, Á.; Horvai, G. *Phys. Chem. Chem. Phys.* **2004**, *6*, 1874.
(53) Pártay, L.; Jedlovszky, P.; Vincze, Á.; Horvai, G. *J. Phys. Chem. B* **2005**, *109*, 20493.
(54) Huiskens, F.; Mohammad-Pooran, S.; Werhahn, O. *Chem. Phys.* **1998**, *239*, 11.

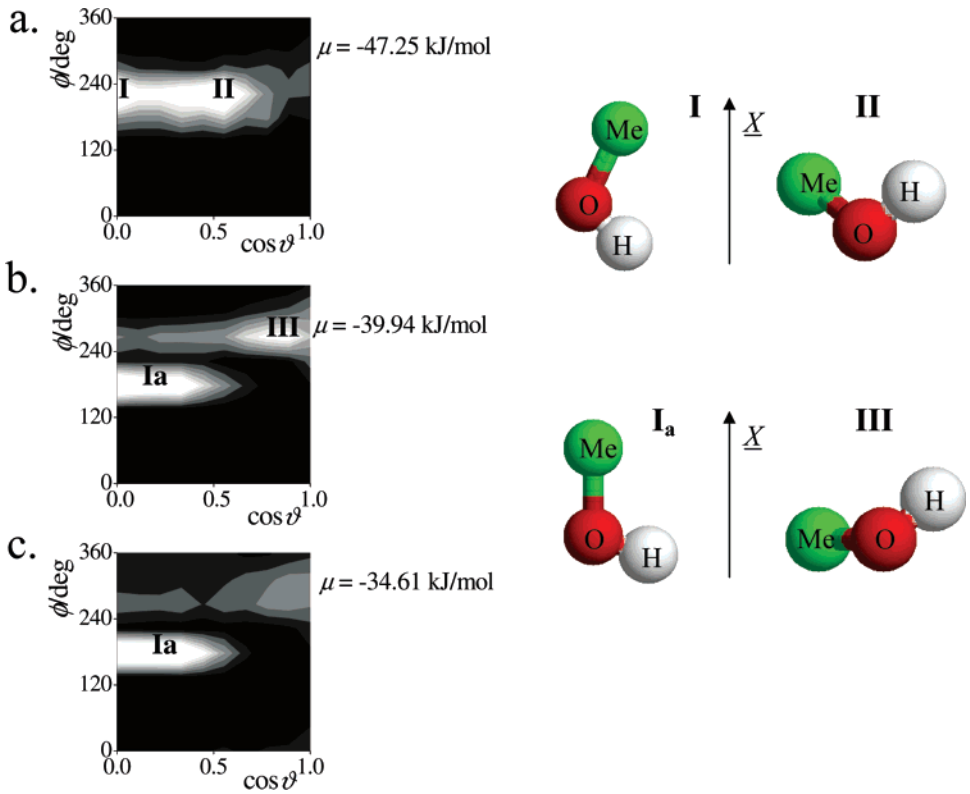

Figure 8. Orientational map of the methanol molecules adsorbed at the ice surface (a) in the system at $\mu = -47.25$ kJ/mol (low surface coverage), (b) in the system at $\mu = -39.94$ kJ/mol (full coverage), and (c) in the first methanol layer of the system at $\mu = -34.61$ kJ/mol (condensed methanol). Lighter gray indicates higher probabilities. The methanol orientations corresponding to the peaks I, I_a, II, and III of the orientational maps are also indicated. $\underline{X}$ is the surface normal vector pointing away from the ice phase.

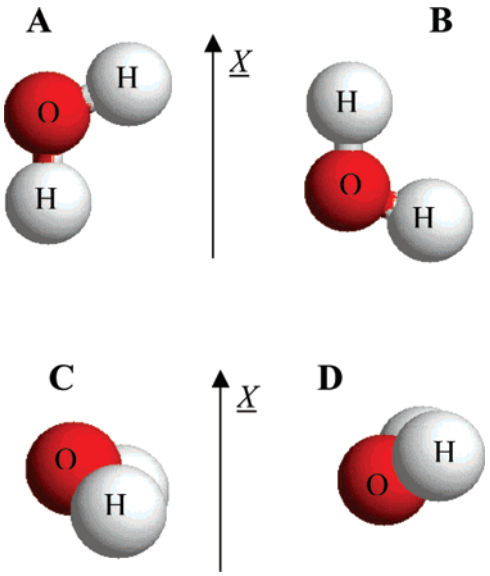

Figure 9. The four possible orientations (A−D) of the water molecules at the free surface of proton-disordered I_h ice. $\underline{X}$ is the surface normal vector pointing away from the ice phase.

orientation II can only form one hydrogen bond with waters, i.e., as an H-acceptor with a water of orientation B (Figure 10). The changes in the orientational preferences of the methanol molecules occurring with the saturation of the adsorption layer, evidenced by the shift of peaks I and II of the $P(\cos\vartheta,\phi)$ orientational map to I_a and III, respectively, are governed by the increasing importance of the formation of stable methanol−methanol hydrogen bonds. Such a hydrogen bond can indeed be formed between a methanol of orientation I_a (as the H-acceptor) and another methanol of orientation III (as the H-donor), both being in the first layer of methanol, as illustrated in Figure 10. The observed weakening of the water−methanol hydrogen bonds upon saturation (Figure 6) is caused by the distortion of its geometry due to the change of the preferred methanol orientation from I to I_a. On the other hand, the weak methanol−methanol hydrogen bonds observed at low coverage are the consequence of the fact that, although the methanol orientations preferred in this case (i.e., I and II) also correspond to the orientation of a hydrogen-bonded methanol pair, such a methanol pair is not lying in a plane parallel with the ice surface; instead, the molecule in orientation I is considerably farther from the surface than that in orientation II. However, the adsorbed methanol molecules are restricted to be in a plane parallel with the ice surface (i.e., in the plane of the adsorption layer), and hence any hydrogen bond between adsorbed methanols of orientations I and II can only be of rather distorted geometry, and consequently rather weak. This distortion is reflected in the fact that intermediate methanol orientations between I and II occur also with high probabilities (Figure 8a). Finally, the disappearance of peak III in the case of condensed methanol can be explained by the fact that, here, the molecules of the first methanol layer are not restricted to form a hydrogen bond with another methanol molecule of the same layer, but instead, they can easily form hydrogen bonds with methanols located farther from the ice surface as well. This possibility largely eliminates the special importance of alignment III in the hydrogen-bonding pattern of the surface methanol molecules.

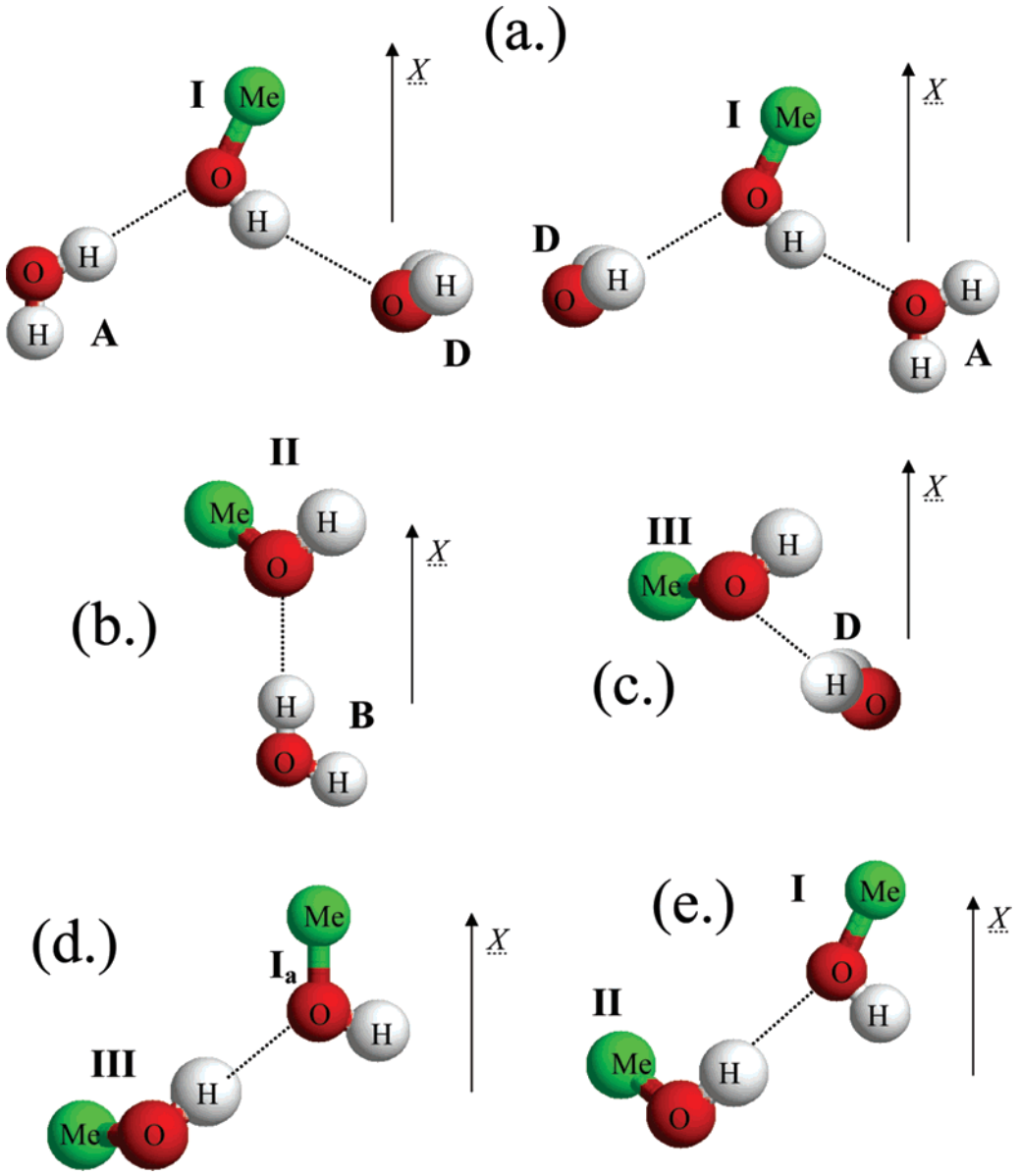

Figure 10. Possible hydrogen bonds between the water molecules located at the ice surface and adsorbed methanol molecules aligned in one of their preferred orientations. (a) A methanol molecule of orientation I is forming two hydrogen bonds with waters of either A- or D-type orientation. (b) A methanol molecule of orientation II is forming a hydrogen bond with a B-type water. (c) A methanol molecule of orientation III is forming a hydrogen bond with a D-type water. (d) A hydrogen bond is formed between a methanol molecule of orientation I_a and another one of orientation III, both belonging to the first methanol layer at the ice surface. (e) A hydrogen bond is formed between a methanol molecule of orientation I and another one of orientation II; however, here the latter methanol is located considerably farther from the ice surface than the former one. $\underline{X}$ is the surface normal vector pointing away from the ice phase.

4. Summary and Conclusions

In this paper, we have presented a combined experimental and computer simulation study of the adsorption of methanol on the surface of ice at 200 K. This study clearly demonstrates the power of combining experimental methods with computer simulation: on one hand, the simulation results can provide a deeper insight into the molecular-level structure and energetics of the adsorption layer than any experiment can do, whereas, on the other hand, the relevance of the simulation results can only be improved and verified by comparison with the experimental data.

In analyzing the properties of the adsorption layer, we have found that its molecular-level structure clearly changes upon saturation. At low surface coverage, the adsorption is driven by the interaction of the adsorbed methanol molecules with the ice phase. Thus, the majority of the methanol molecules form two hydrogen bonds with waters (i.e., one as an H-donor and another one as an H-acceptor) but have no hydrogen-bonded methanol neighbors. This is also reflected in the preferred surface orientations of the methanol molecules. In one of these preferred orientations, methanol can form two hydrogen bonds with the surface water molecules, but the two preferred methanol orientations correspond only to an off-plane hydrogen-bonded pair, and consequently any hydrogen bond between two methanols located at the plane of the adsorption layer must be rather distorted and thus rather weak. On the other hand, upon saturation, the methanol−methanol interactions become as important as the methanol−water ones: at full coverage, roughly half of the methanol molecules form one hydrogen bond with a water neighbor and another one with a methanol neighbor,

whereas the other half of them have two hydrogen-bonded water neighbors and one methanol neighbor. Correspondingly, upon saturation, one of the preferred surface orientations of the methanol molecules changes completely, and the other one slightly, in order to enable the methanols to form stable hydrogen bonds with each other within the plane of the adsorption layer, at the expense of weakening the methanol−water hydrogen bonds.

Finally, it should be noted that the observed surface orientations of the methanol molecules is completely different from what we have observed at the liquid−vapor interface of water−methanol mixtures, in spite of the fact that methanol shows a strong tendency for surface adsorption in such systems.[53] On the other hand, this behavior is rather similar to that of 1-octanol[55] and triethoxy-monooctyl ether[56] at the air−water interface, probably due to the fact that, in these systems, similarly to the presently studied one, the adsorbed molecules are completely separated from the phase containing the water molecules, whereas at the surface of liquid water−methanol mixtures the two molecules mix with each other, allowing hydrogen-bonding between the molecules in a much wider variety of orientations.

Acknowledgment. This work has been supported by the Hungarian−French Intergovernmental Science and Technology Program (BALATON) under project no. F/33-04, by the MTA−CNRS bilateral collaboration program, and partly by the Hungarian OTKA Foundation under project no. T049673. P.J. is a Békésy György fellow of the Hungarian Ministry of Education, which is gratefully acknowledged. The authors are grateful to Albert Bartók for providing the coordinates of the molecules in the ice I_h crystal. The experimental work was carried out within the framework of the EU sixth framework project "SCOUT-O_3".

Supporting Information Available: Complete ref 4. This material is available free of charge via the Internet at http://pubs.acs.org.

JA065553+

(55) Jedlovszky, P.; Varga, I.; Gilányi, T. *J. Chem. Phys.* **2004**, *120*, 11839.
(56) Paszternák, A.; Kiss, E.; Jedlovszky, P. *J. Chem. Phys.* **2005**, *122*, 124704.